

CONF-800723--16

19th National Heat Transfer Conference

July 27-30, 1980

Orlando, Florida

**MASTER**

AN ANALYSIS OF MOLTEN DEBRIS FREEZING AND WALL EROSION  
DURING A SEVERE RIA TEST

Mohamed S. El-Genk and Richard L. Moore

Idaho National Engineering Laboratory  
EG&G Idaho, Inc.  
P.O. Box 1625  
Idaho Falls, Idaho 83415

DISCLAIMER

This book was prepared as an account of work sponsored by an agency of the United States Government. Neither the United States Government nor any agency thereof, nor any of their employees, makes any warranty, express or implied, or assumes any legal liability or responsibility for the accuracy, completeness, or usefulness of any information, apparatus, product, or process disclosed, or represents that its use would not infringe privately owned rights. Reference herein to any specific commercial product, process, or service by trade name, trademark, manufacturer, or otherwise, does not necessarily constitute or imply its endorsement, recommendation, or favoring by the United States Government or any agency thereof. The views and opinions of authors expressed herein do not necessarily state or reflect those of the United States Government or any agency thereof.

DISTRIBUTION OF THIS DOCUMENT IS UNLIMITED

## **DISCLAIMER**

**This report was prepared as an account of work sponsored by an agency of the United States Government. Neither the United States Government nor any agency Thereof, nor any of their employees, makes any warranty, express or implied, or assumes any legal liability or responsibility for the accuracy, completeness, or usefulness of any information, apparatus, product, or process disclosed, or represents that its use would not infringe privately owned rights. Reference herein to any specific commercial product, process, or service by trade name, trademark, manufacturer, or otherwise does not necessarily constitute or imply its endorsement, recommendation, or favoring by the United States Government or any agency thereof. The views and opinions of authors expressed herein do not necessarily state or reflect those of the United States Government or any agency thereof.**

## **DISCLAIMER**

**Portions of this document may be illegible in electronic image products. Images are produced from the best available original document.**

## CONTENTS

ABSTRACT . . . . .	1
1. INTRODUCTION. . . . .	1
2. EXPERIMENT DESCRIPTION, CONDUCT, AND RESULTS. . . . .	3
3. PHYSICAL MODEL. . . . .	6
4. ANALYSIS. . . . .	9
5. RESULTS AND DISCUSSION. . . . .	13
5.1. Potential Wall Erosion Due to Melting. . . . .	19
5.2. Accuracy of the Finite Element Computer Code SINGLE. . .	24
6. SUMMARY AND CONCLUSIONS . . . . .	24
7. REFERENCES. . . . .	28
NOMENCLATURE . . . . .	30
NO. OF TABLES. . . . .	3
NO. OF FIGURES . . . . .	10

AN ANALYSIS OF MOLTEN DEBRIS FREEZING AND WALL EROSION  
IN A SEVERE RIA TEST\*

Mohamed S. El-Genk and Richard L. Moore

EG&G Idaho, Inc.  
P.O. Box 1625  
Idaho Falls, ID 83415

ABSTRACT

A one-dimensional physical model was developed to study the transient freezing of the molten debris layer (a mixture of  $UO_2$  fuel and zircaloy cladding) produced in a severe reactivity initiated accident in-pile test and deposited on the inner surface of the test shroud wall. The wall had a finite thickness and was cooled along its outer surface by coolant bypass flow. Analyzed are the effects of debris temperature, radiation cooling at the debris layer surface, zircaloy volume ratio within the debris, and initial wall temperature on the transient freezing of the debris layer and the potential melting of the wall. The governing equations of this two-component, simultaneous freezing and melting problem in a finite geometry were solved using a one-dimensional finite element code based on the method of weighted residuals.

1. INTRODUCTION

A concern in assuring the safety of commercial light water reactors (LWRs) is to understand the transient freezing of the core molten debris, which is primarily a mixture of  $UO_2$  fuel and zircaloy cladding, on cold core structures following a hypothetical core meltdown accident (HCMA). The analysis of such non-design-base accidents in LWRs was encouraged by the NRC in response to the Three Mile Island-2 (TMI-2) accident. The purpose of this paper is to study the transient freezing of the molten debris layer produced and

---

\* This work was supported by the U. S. Nuclear Regulatory Commission, Division of Fuel Behavior Research.

deposited on the inner surface of the test shroud cold wall during a severe reactivity initiated accident experiment (RIA-ST-4), and to assess the potential erosion of the wall due to melting upon being contacted by the molten debris.

The RIA-ST-4 experiment<sup>1</sup> was composed of a single, unirradiated, 20 wt% enriched  $UO_2$  fuel rod contained within a zircaloy flow shroud. The test rod was subjected to a single power burst which deposited a total energy of about 700 cal/g  $UO_2$ , simulating a severe boiling water reactor (BWR) control rod ejection accident from hot startup conditions. This energy deposition is well above what is possible in a commercial LWR during postulated control rod ejection (from the bottom of a BWR or the top of a PWR) accidents. However, the performance of such an in-pile experiment<sup>1</sup> has provided important information regarding molten debris movement, relocation, and freezing on cold walls.

Extensive amounts of molten fuel and cladding were produced and ejected axially and radially within the test shroud upon rod failure. The generation of pressure pulses up to 35 MPa indicated rod failure at about 33 ms after the initiation of the power burst. Upon fuel rod failure, a debris layer having a thickness of about 0.7 mm was deposited on the inner surface of the test shroud wall. The shroud wall had a thickness of 3.05 mm and was continuously cooled at its outer surface by coolant bypass flow.

The purpose of the present work was to develop a physical model (described in Section 3) to study the transient freezing of the molten debris layer deposited on the inner surface of the RIA-ST-4 shroud wall. The governing equations were solved using a one-dimensional, finite element computer code (SINGLE), based on the method of weighted residuals.<sup>2</sup> The analysis considered the conditions of finite wall thickness, continuous cooling at the wall outer surface, radiation cooling at the molten debris layer surface, internal heat generation in the debris, and temperature-dependent thermophysical properties. Discussed are the effects of molten debris temperature, radiation

cooling, zircaloy volume ratio within the debris, and initial wall temperature on the transient freezing of the debris layer and the potential erosion of the wall due to melting.

## 2. EXPERIMENT DESCRIPTION, CONDUCT, AND RESULTS

The RIA-ST-4 experiment was one of four scoping tests in the RIA test series which is being conducted in the Power Burst Facility at the Idaho National Engineering Laboratory to define an energy deposition failure threshold and to determine the modes and consequences of fuel rod failure during a postulated boiling water reactor (BWR) control rod ejection accident. These RIA tests are being performed at typical BWR hot startup conditions (coolant pressure of 6.46 MPa, coolant temperature of 538 K, and coolant flow rate through the test shroud of 0.085 l/s). The objective of the RIA-ST-4 experiment was to quantify the magnitude of potential pressure pulses as a result of fuel rod failure during severe RIA conditions. Figure 1 presents an axial cross section of the RIA-ST-4 test fuel rod assembled in the test shroud. Table 1 lists the test fuel rod and the shroud design characteristics. Details of test instrumentation and experimental results are described elsewhere.<sup>1</sup>

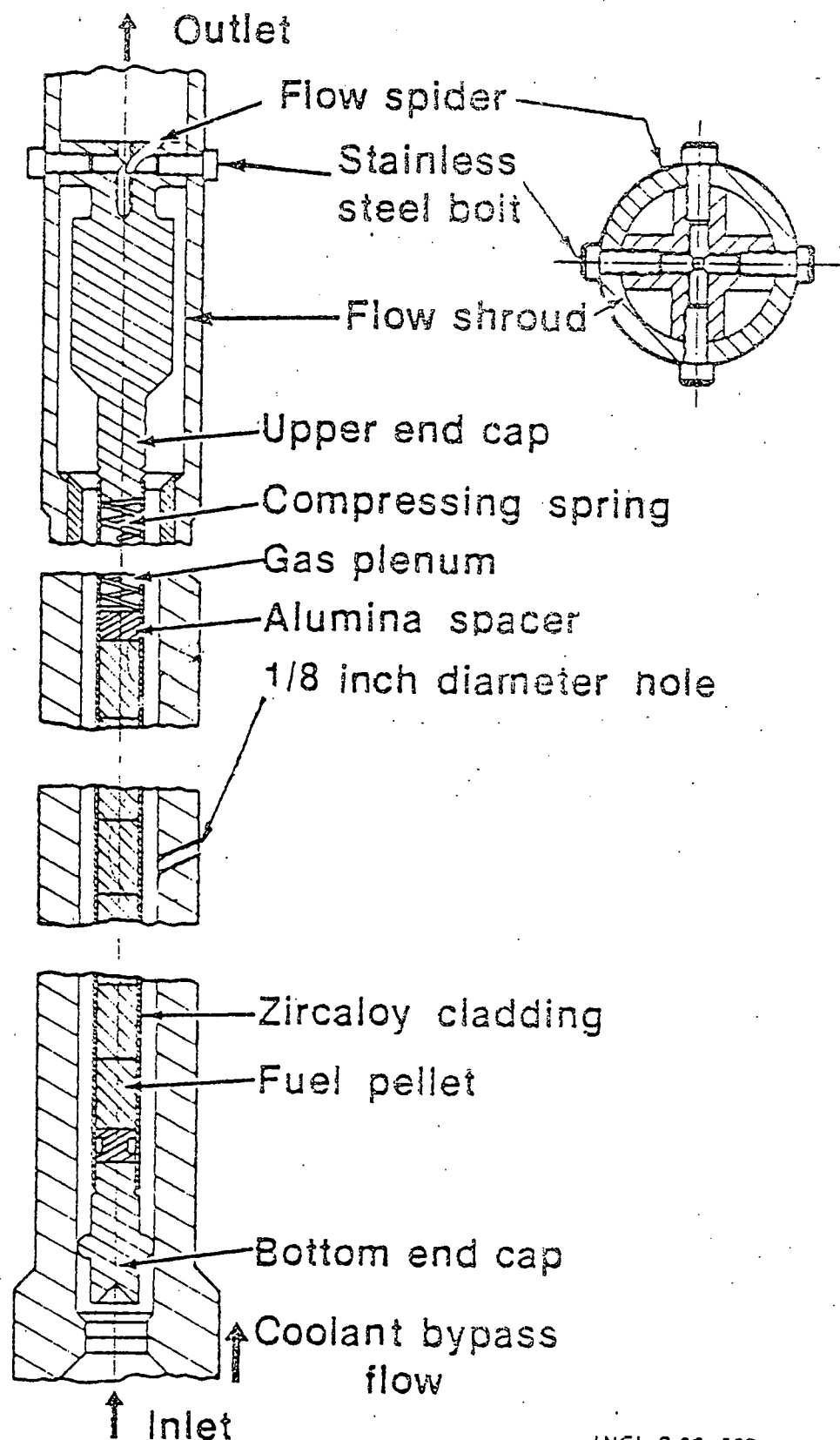
TABLE 1. DESIGN CHARACTERISTICS OF THE RIA-ST-4 TEST FUEL ROD AND FLOW SHROUD

### Fuel Rod

Overall length (m)	1.0
Material (%TD)	UO <sub>2</sub> (93)
Enrichment (wt%)	20
Burnup	Unirradiated
Cold internal pressure (MPa)	3.79
Rod OD (mm)	10.73
Cladding	Zr-4
Cladding thickness (mm)	0.61
Diametral gap width (mm)	0.105

### Flow Shroud

Material	Zircaloy-4
ID (mm)	19.3
Wall thickness (mm)	3.05
Coolant inlet velocity (m/s)	~0.42
Coolant bypass flow (l/s)	~0.10



INEL-S-22 537

Figure 1. Axial cross section of the RIA-ST-4 test fuel rod assembled in the test shroud.

In the RIA-ST-4 experiment, a single  $UO_2$  fuel rod contained within a zircaloy flow shroud was subjected to a single power burst, resulting in a total energy deposition of about 700 cal/g  $UO_2$ . A reactor peak power of about 15.9 GW was achieved approximately 30 ms after the initiation of the burst, which lasted a total of about 76 ms. The test fuel rod failed 3 ms after the reactor peak power occurred, at which time the total energy deposition was about 370 cal/g  $UO_2$ . The generation of coherent pressure pulses up to 35 MPa, due to molten fuel-coolant interaction<sup>3</sup> (vapor explosion), indicated rod failure. The average temperature of the fuel at the time of failure was estimated to have been about 3500 K ( $\approx 400$  K above the  $UO_2$  melting point). At this temperature the contribution to the generated pressure by the  $UO_2$  fuel vapor was negligibly small, about 0.05 MPa. The coolant temperature at the exit of the flow shroud reached values in excess of 940 K, which is much higher than the critical temperature of the coolant ( $T_{crit} = 647$  K).

At the time of the test rod failure, extensive amounts of molten  $UO_2$  fuel and zircaloy cladding were produced and expelled axially and radially within the flow shroud due to the high internal pressure in the test rod. Molten debris that was ejected upward froze, forming a complete flow blockage at the exit of the flow shroud and causing erosion of the flow spider (Figure 1) due to melting. The inner surface of the shroud wall was coated with a debris layer having a thickness of 0.7 mm. However, the inner surface of the wall did not melt when contacted by the molten debris. The amount of molten debris deposited on the inner surface of the shroud wall was about 380 g, which represents 57% of the total mass of  $UO_2$  fuel and zircaloy cladding in the test rod. The following section discusses a physical model developed to study the transient freezing of the molten debris layer deposited on the inner surface of the test shroud wall.

### 3. PHYSICAL MODEL

A schematic representation of the physical model is in Figure 2. At time zero (fuel rod failure time), a molten debris layer having a thickness 'a' was plated on the inner surface of the shroud wall,  $r = 0$ . The shroud wall had a finite thickness 'b' and was initially at a uniform temperature equal to that of the coolant bypass flow,  $T_c$ , at the wall outer surface,  $r = -b$ . The initial molten debris temperature,  $T_D$ , was higher than the fusion temperature of the  $UO_2$  fuel ( $T_{f_{UO_2}} = 3113$  K) and the freezing temperature of the zircaloy cladding ( $T_{f_{Zr}} = 2100$  K). Should the temperature, of the interface,  $T_I(t)$ , between the shroud wall and the molten debris layer reach a value in excess of the melting point of the wall ( $T_{mp} = 2100$  K), then freezing of the molten debris and simultaneous melting of the wall would occur. Otherwise, only freezing of the molten debris layer occurs.

During the freezing process, the heat transmission through the debris layer,  $0 \leq r \leq a$ , was controlled by two means. First, by the transient heat conduction through the shroud wall, which had a finite thickness and was continuously cooled at its outer surface, and secondly, by the transient radiation cooling at the debris layer surface,  $r = a$ , to the water vapor within the flow shroud. These cooling mechanisms strongly influence the heat transmission within the debris because of the small thickness of the debris layer. Therefore, the contribution to the effective thermal conductivity of the debris by the internal electromagnetic radiation within the debris layer is neglected. However, for those cases in which the debris layer is thicker, the internal electromagnetic radiation, far from the boundaries, would be important because of the porosity of the  $UO_2$  fuel.<sup>4</sup>

The fission heating within the molten debris (from the time of fuel rod failure until the end of the power burst—about 45 ms) was accounted for through the use of a rate law of the form

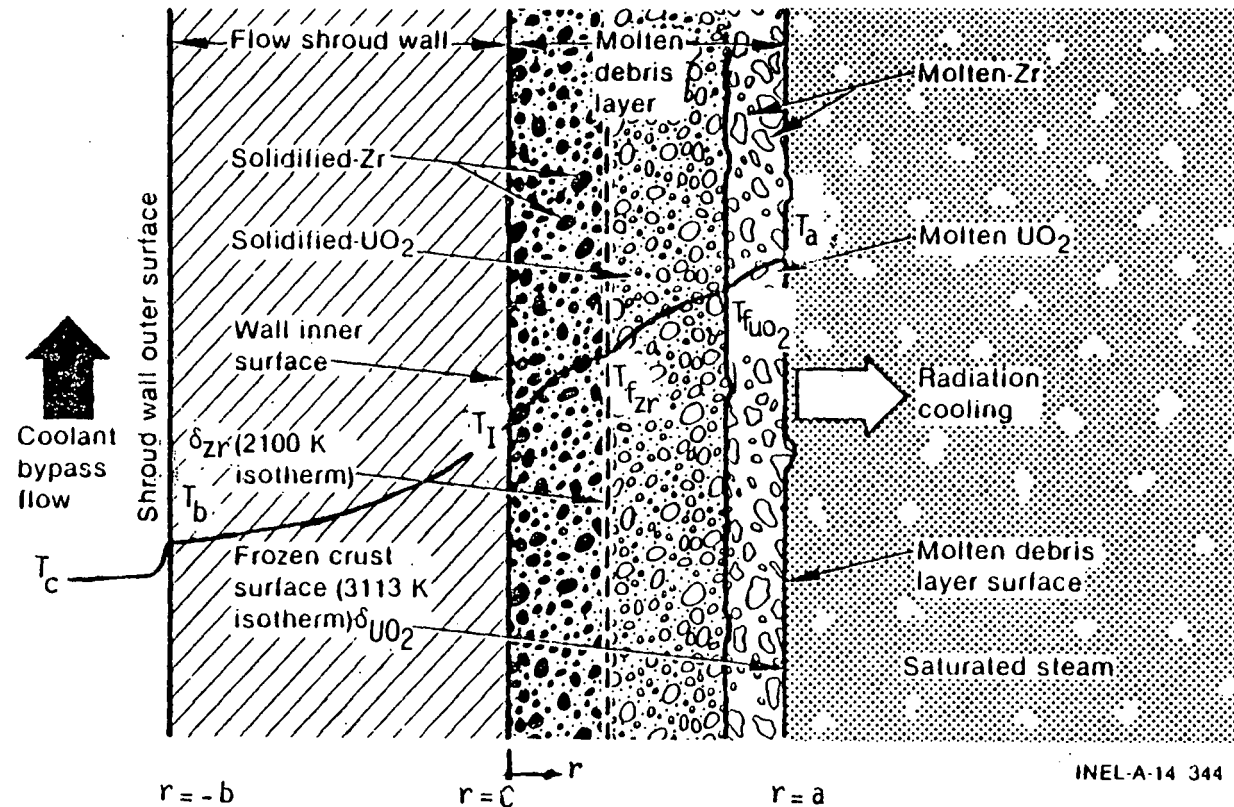


Figure 2. Physical model.

INEL-A-14 344

TABLE 2. BOUNDARY AND INITIAL CONDITIONS IN THE WALL ( $-b \leq r \leq 0$ )

Item	Without Simultaneous Melting of the Wall	With Simultaneous Melting of the Wall
Boundary Conditions	$k_w \frac{\partial T_w}{\partial r} (0, t) = k_s \frac{\partial T_s}{\partial r} (0, t)$ $k_w \frac{\partial T_w}{\partial r} (-b, t) = h_c (T_b - T_c), \text{ if } T_b < T_{crit}$ $k_w \frac{\partial T_w}{\partial r} (-b, t) = h_B (T_b - T_c), \text{ if } T_b \geq T_{crit}$ $T_w (0, t) = T_I (t)$	<p>(a) <u>In the Solid Region of the Wall (<math>-b \leq r \leq -\delta_m</math>)</u></p> $k_w \frac{\partial T_w}{\partial r} (-\delta_m, t) = k_m \frac{\partial T_m}{\partial r} (-\delta_m, t) - \rho_w L_m \frac{d\delta_m}{dt}$ The same The same $T_w (-\delta_m, t) = T_{imp}$
Initial Conditions	$T_w (-r, 0) = T_c$	<p>(b) <u>In the Wall Molten Layer (<math>-\delta_m &lt; r &lt; 0</math>)</u></p> $k_m \frac{\partial T_m}{\partial r} (0, t) = k_s \frac{\partial T_s}{\partial r} (0, t)$ $T_m (-\delta_m, t) = T_{imp}$ $T_m (0, t) = T_I (t)$ The same $\delta_m (t = 0) = 0$

$$Q(t) = Q_0 \text{ Exp } (-Bt) \quad (1)$$

where  $B$  is a time constant that governs the fission heating decay rate ( $\sim 110 \text{ s}^{-1}$ ) within the debris.

The effective thermophysical properties of the debris were assessed in terms of those of the  $\text{UO}_2$  fuel and of the zircaloy cladding as follows.

### Density

$$\rho_s = \rho_{\text{Zr}} \epsilon + \rho_{\text{UO}_2} (1 - \epsilon) \quad (2)$$

### Heat capacity

$$C_s = \frac{1}{\rho_s} \left[ \rho_{\text{Zr}} C_{\text{Zr}} \epsilon + \rho_{\text{UO}_2} C_{\text{UO}_2} (1 - \epsilon) \right], \quad (3)$$

and

### Thermal conductivity<sup>5</sup>

$$k_s = k_{\text{UO}_2} \left\{ \frac{2 + (k_{\text{Zr}}/k_{\text{UO}_2}) - 2 \epsilon [1 - (k_{\text{Zr}}/k_{\text{UO}_2})]}{2 + (k_{\text{Zr}}/k_{\text{UO}_2}) + \epsilon [1 - (k_{\text{Zr}}/k_{\text{UO}_2})]} \right\} \quad (4)$$

where  $\epsilon$  is the zircaloy volume ratio within the debris, and the subscript  $s$  refers to the debris.

## 4. ANALYSIS

In the current study, the molten debris is treated as a homogeneous mixture of  $\text{UO}_2$  fuel and zircaloy cladding, with volume ratios equivalent to those of the test fuel rod before the burst ( $\sim 13\%$  zircaloy and  $87\% \text{UO}_2$ ). Therefore, the freezing of the molten debris layer is completed through two successive stages. In the first stage, the molten  $\text{UO}_2$  freezes as the temperature in the molten debris drops

below the melting point of  $UO_2$  fuel (3113 K). Next, the molten zircaloy within the  $UO_2$  fuel crust (which froze in the first stage) freezes when the temperature in the crust drops below the melting point of zircaloy (2100 K). As shown in Figure 2, two moving fronts with a change-of-phase are formed within the molten debris layer (that is,  $r = \delta_{UO_2}$  and  $r = \delta_{Zr}$ ). The advanced front,  $r = \delta_{UO_2}$ , corresponds to a temperature isotherm equal to the melting point of  $UO_2$ , and the second front,  $r = \delta_{Zr}$ , represents the melting point of zircaloy.

The transient heat conduction equation in the debris layer ( $0 \leq r \leq a$ ) is of the general form

$$\rho(T) C(T) \frac{\partial T}{\partial t} = \frac{1}{r} \frac{\partial}{\partial r} [r k(T) \frac{\partial T}{\partial r}] + \frac{Q(t)}{\rho} \quad (5)$$

where  $Q(t)$  is a fission heating rate (W/g) defined by Equation (1).

The boundary conditions at the change-of-phase front,  $r = \delta_{Zr}$ , and the solidification front,  $r = \delta_{UO_2}$ , are

$$k_s \frac{\partial T_s}{\partial r} (\delta_{Zr}, t) = k_s \frac{\partial T_s}{\partial r} [(a - \delta_{Zr}), t] + \epsilon \rho_{Zr} L_{Zr} \frac{d\delta_{Zr}}{dt} \quad (6)$$

$$T_s (\delta_{Zr}, t) = T_s [(a - \delta_{Zr}), t] = T_{f_{Zr}} \quad (7)$$

$$k_s \frac{\partial T_s}{\partial r} (\delta_{UO_2}, t) = k_s \frac{\partial T_s}{\partial r} [(a - \delta_{UO_2}), t] + (1 - \epsilon) \rho_{UO_2} L_{UO_2} \frac{d\delta_{UO_2}}{dt} \quad (8)$$

$$T_s (\delta_{UO_2}, t) = T_s [(a - \delta_{UO_2}), t] = T_{f_{UO_2}} \quad (9)$$

The boundary condition at the molten debris layer surface,  $r = a$ , is

$$k_s \frac{\partial T_s}{\partial r} (a, t) = h_R [T_a (t) - T_{sat}] \quad (10)$$

and the initial conditions are that  $\delta_{Zr}(t = 0) = 0$ ,  $\delta_{UO_2}(t = 0) = 0$  and  $T_s(r, 0) = T_D$ , where  $T_D$  is the molten debris temperature at the time of test rod failure.

In Equation (10) the radiation cooling heat transfer coefficient,  $h_R$ , at the debris layer surface,  $r = a$ , can be generally expressed as

$$h_R = \frac{\sigma_s B}{\frac{1}{\epsilon_f} + \frac{1}{\epsilon_v} - 1} \left[ \frac{T_a^4(t) - T_{sat}^4}{T_a(t) - T_{sat}} \right] \quad (11)$$

where,  $\epsilon_f$  and  $\epsilon_v$  are the thermal emissivities of the  $UO_2$  fuel and of the water vapor, respectively, and  $T_a(t)$  is the temperature of the debris layer surface,  $r = a$ . The thermal emissivity of the fuel,  $\epsilon_f$ , was taken to be constant and equal to 0.4083.<sup>6</sup> A value of 0.18 for  $\epsilon_v$  was evaluated (using the figures given in Reference 7) at an average vapor temperature equal to the arithmetic average of the saturated temperature of the vapor (544 K), corresponding to the system pressure (6.45 MPa), and the temperature of the molten debris,  $T_D$  at the time of failure.

The transient heat conduction equation in the wall ( $-b \leq r \leq 0$ ) is of the general form

$$\rho(T) C(T) \frac{\partial T}{\partial t} = \frac{1}{r} \frac{\partial T}{\partial r} \left[ r k(T) \frac{\partial T}{\partial r} \right] \quad (12)$$

and the boundary and initial conditions are as listed in Table 2. As shown in Table 2, two modes of heat transfer were considered to occur at the shroud wall outer surface during the freezing process of the debris, namely, a forced convection heat transfer and a stable film boiling heat transfer. The convective coefficient of heat transfer,  $h_c$ , can be obtained through use of the Dittus-Boelter correlation

$$\frac{h_c D}{k_1} = 0.023 \left( \frac{\rho_1 D v}{\mu_1} \right)^{0.8} \left( \frac{\mu_1 C_1}{k_1} \right)^{0.4} \quad (13)$$

where the thermophysical properties of the coolant ( $\rho_1$ ,  $k_1$ ,  $C_1$  and  $\mu_1$ ) were evaluated at the coolant bulk temperature (538 K).

Stable film boiling was assumed to commence as soon as the temperature at the shroud wall outer surface reached or exceeded the critical temperature of the coolant ( $T_{crit} = 647$  K). The stable film boiling heat transfer coefficient,  $h_B$ , is given through use of the following relations proposed by Bromley:<sup>8</sup>

$$h_B = h_{co} + 0.75 h_r, \quad \text{when } (h_c > h_r) \quad (14a)$$

and

$$h_B = h_{co} + h_r \left\{ 0.75 + 0.25 \left[ \frac{\left( \frac{h_r}{h_{co}} \right)}{2.62 + \left( \frac{h_r}{h_{co}} \right)} \right] \right\} \quad \text{when } (h_c < h_r) \quad (14b)$$

The term  $h_{co}$  is obtained from the Ellion<sup>9</sup> correlation for film boiling on vertical cylinders

$$h_{co} = 0.714 \left[ \frac{k_v \rho_v \rho_1 h_{fg} g}{H \mu_v (T_b - T_{sat})} \right]^{0.25} \quad (15)$$

The contribution to  $h_B$  by the thermal radiation across the vapor film,  $h_r$ , was accounted for by the following equation for parallel plates:

$$h_r = \frac{\sigma_s B}{\frac{1}{\epsilon_w} + \frac{1}{\epsilon_l} - 1} \left( \frac{T_b^4 - T_c^4}{T_b - T_{sat}} \right) . \quad (16)$$

In the next section the transient freezing process of the molten debris layer on the inner surface of the RIA-ST-4 shroud wall is studied parametrically.

## 5. RESULTS AND DISCUSSION

The governing equations, with the boundary and initial conditions presented in the previous section, were solved numerically using a one-dimensional finite element code (SINGLE) based on the method of weighted residuals.<sup>2</sup> Calculated are the instantaneous values of the functions; namely, the frozen crust thickness,  $\delta_{U_0}(t)$ ; the moving change-of-phase front,  $\delta_{Z_r}(t)$ ; the temperature of the debris layer surface,  $T_a(t)$ ; the temperature of the wall inner surface,  $T_I(t)$ ; and the temperature of the wall outer surface,  $T_b(t)$ . In addition, the instantaneous thickness of the wall molten layer,  $\delta_m(t)$ , was calculated for the cases in which wall melting occurred upon contact with the molten debris. The parameters for the reference case are listed in Table 3 and the calculated results are plotted in Figure 3.

TABLE 3. REFERENCE CASE PARAMETERS

---

Initial molten debris temperature (K)	3500
Zircaloy volume ratio within the debris	0.1282
Debris layer thickness (mm)	0.7
Shroud wall thickness (mm)	3.05
Coolant bypass flow temperature (K)	538
Fission heating rate within the debris at time of rod failure, $Q_0$ (W/g UO <sub>2</sub> )	$8 \times 10^4$

---

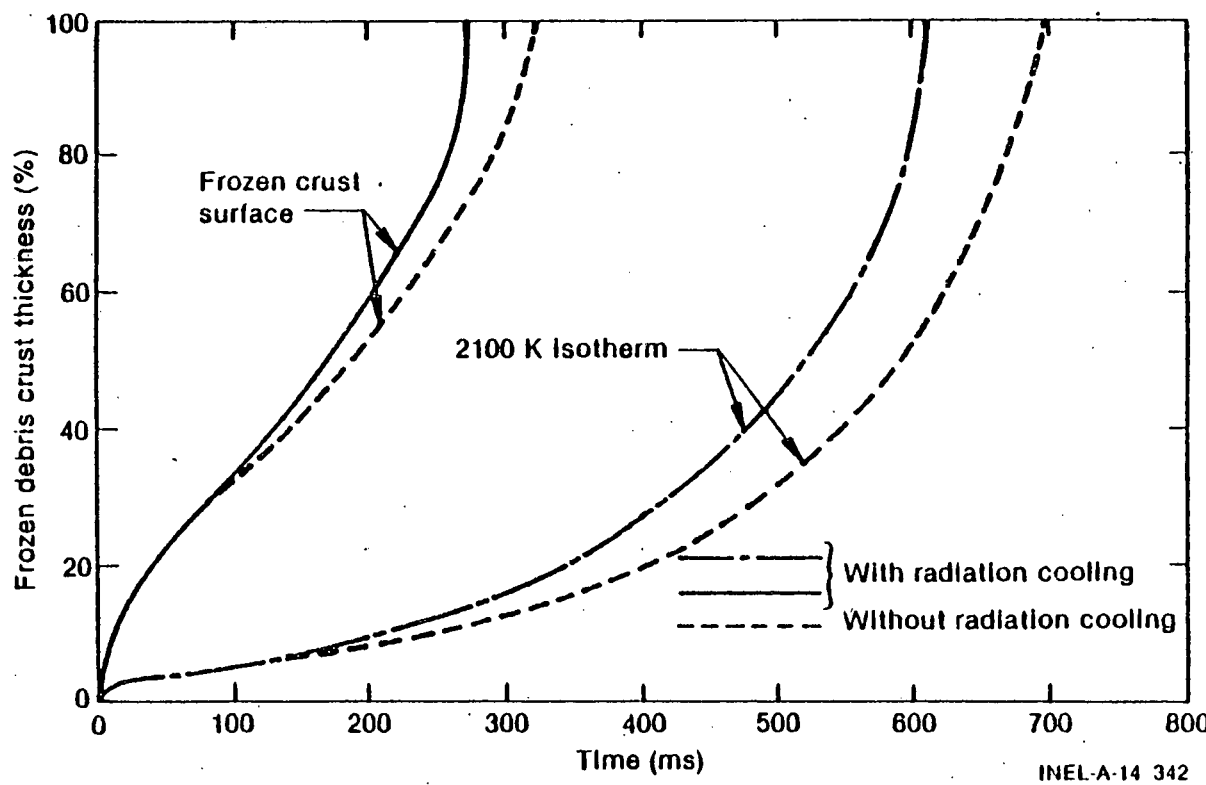


Figure 3. Transient freezing of the molten debris layer on the inner surface of the test shroud wall.

Figure 3 presents a plot of the instantaneous frozen crust thickness as a percentage of the initial thickness of the debris layer. The zero mark on the ordinate represents the inner surface of the shroud wall, and the hundred mark represents the measured debris layer surface. At the initial time of contact, the transient heat conduction through the shroud wall caused the temperature of the wall inner surface,  $T_I$ , to reach a value of about 1870 K, which is less than the melting point of the wall material (2100 K) and the freezing temperature of the  $UO_2$  fuel (3113 K), indicating that no melting of the wall would occur under the conditions listed in Table 3. A solidification front corresponding to the melting point of  $UO_2$  (presented by the solid line in Figure 3) appears at the wall inner surface,  $r = 0$ , moving into the molten debris layer away from wall. Following that, the molten zircaloy within the  $UO_2$  solidified crust freezes when the temperature within the crust drops below the melting point of the zircaloy (2100 K). As indicated, the transient freezing of the debris is influenced by the radiation cooling at the molten debris layer surface, which speeds up the freezing process and thus reduces the total freezing time of the molten debris layer.

Figure 4 demonstrates the effect of the initial molten debris temperature,  $T_D$ , on the transient freezing of the debris layer. As shown, increasing the molten debris temperature slows down the freezing process, and thus increases the total freezing time of the molten debris layer. For instance, increasing the initial debris temperature from 3500 to 5000 K results in a two-fold increase of the total freezing time.

The calculated temperature-time histories at the shroud wall inner and outer surfaces are plotted in Figures 5 and 6, respectively. Time zero is the time at which the inner surface of the wall was contacted by the molten debris. As shown in Figure 6, film boiling commenced at the shroud wall outer surface (that is, when  $T_b \geq 647$  K) very shortly after the time of contact, causing wall overheating and oxidation of the shroud wall outer surface due to the steam-zircaloy reaction.<sup>10-11</sup> The maximum temperature at the outer

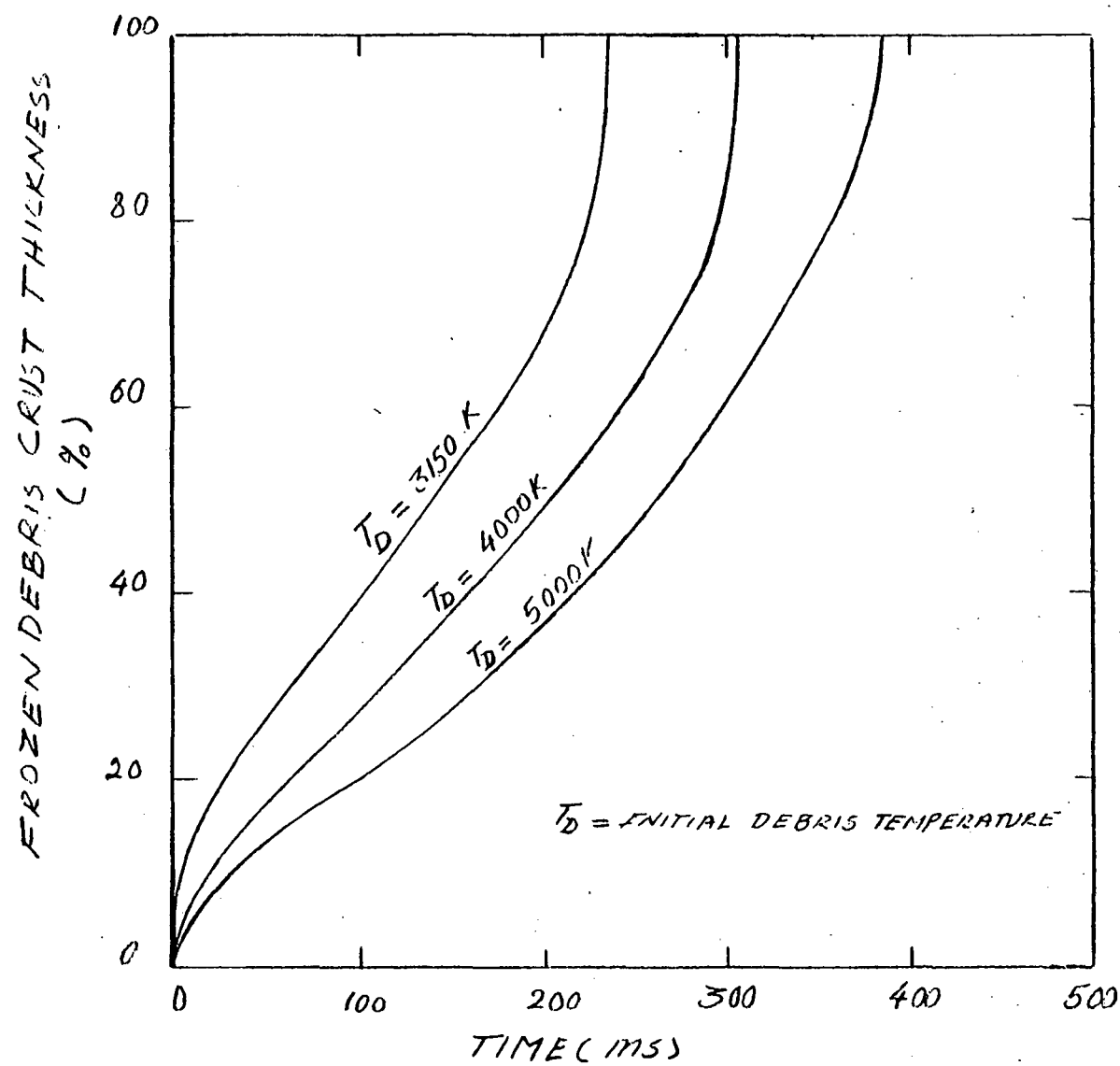


Figure 4. Effect of molten debris temperature on the transient freezing of the debris layer.

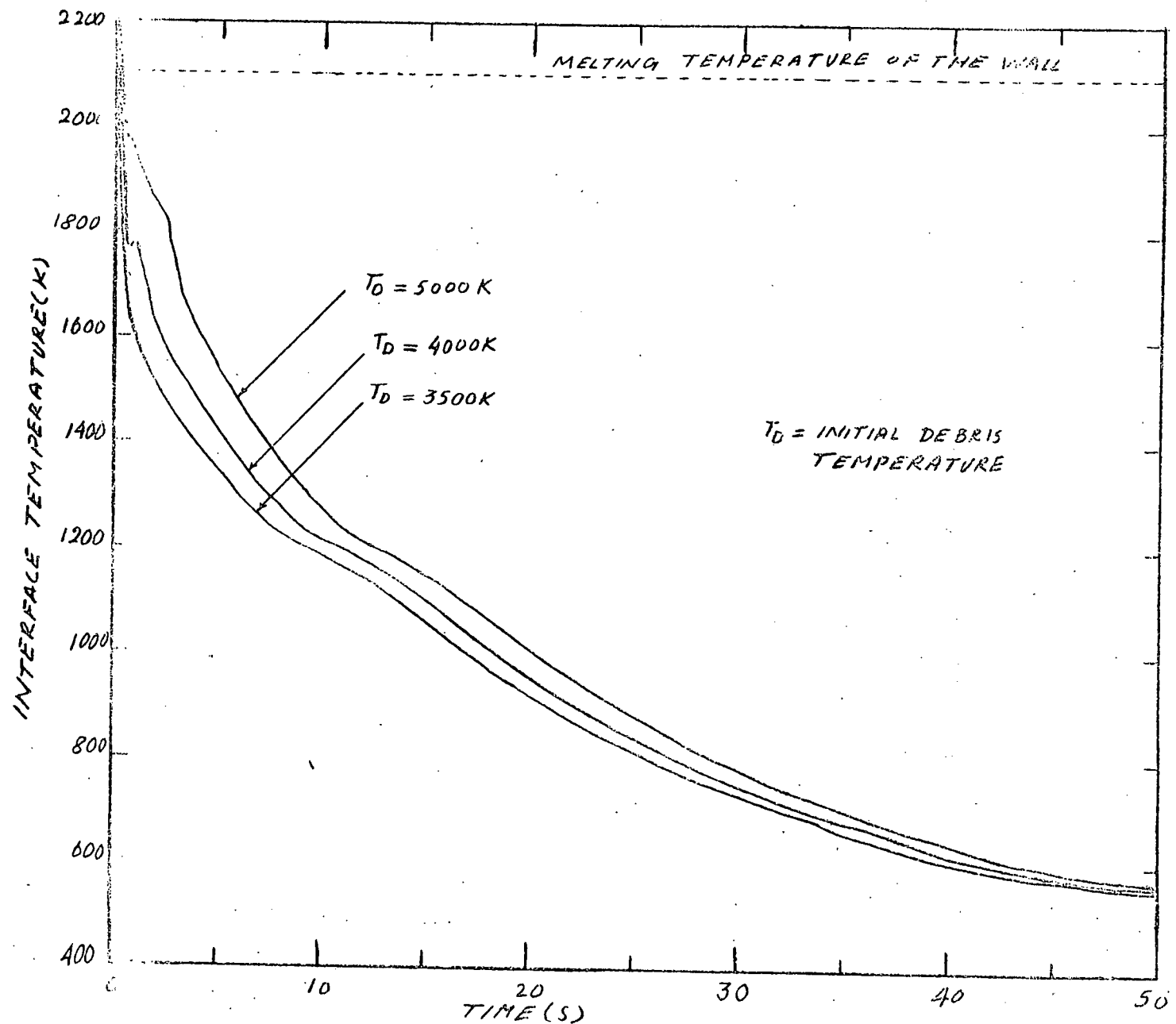


Figure 5. Temperature-time history at the shroud wall inner surface.

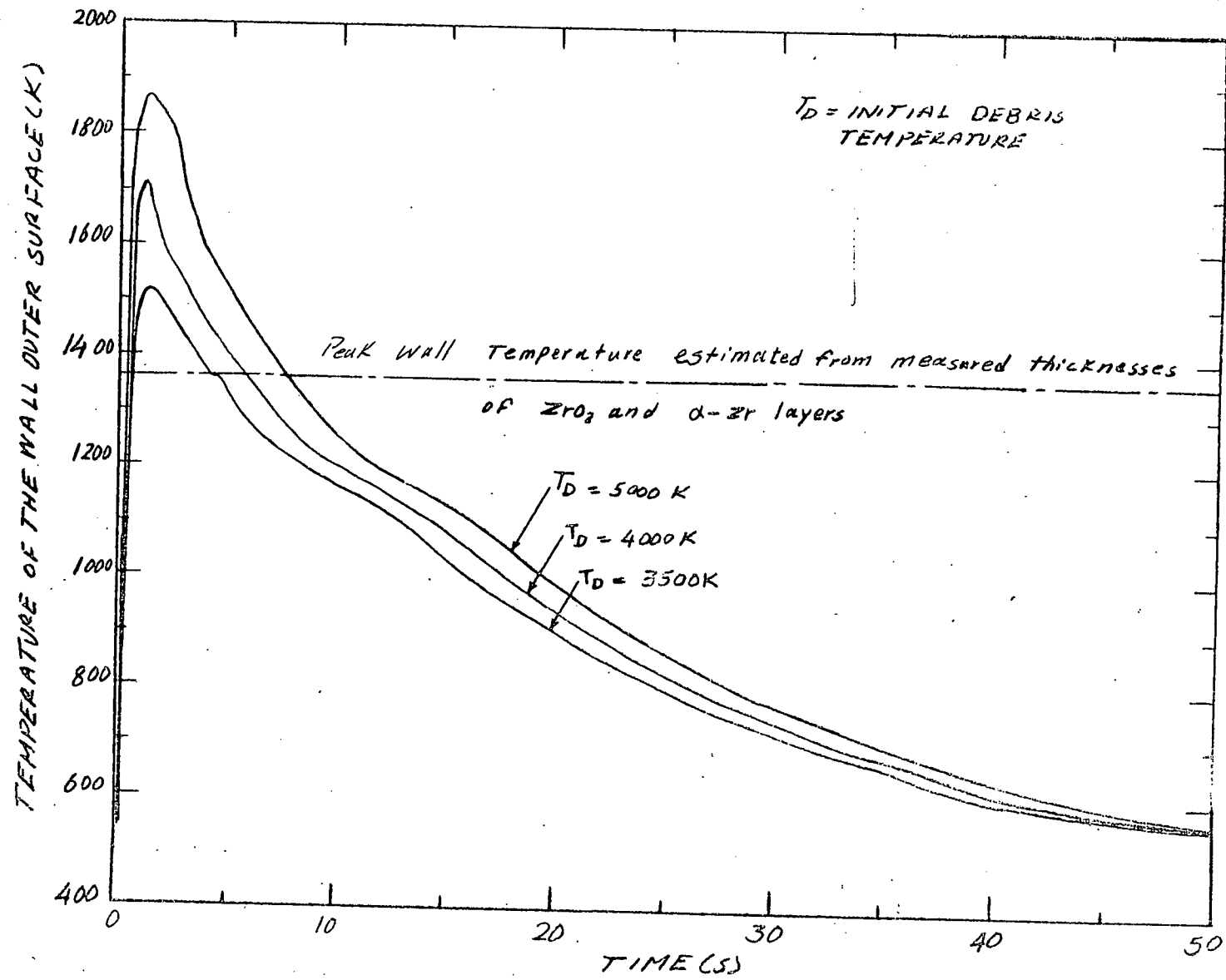


Figure 6. Temperature-time history at the shroud wall outer surface.

surface of the wall increases as the initial molten debris temperature is increased. For example, increasing the molten debris temperature from 3500 to 4000 K increases the maximum temperature at the wall outer surface from 1520 to 1580 K, without significant change in the duration of film boiling. The horizontal broken line in Figure 6 represents the wall surface peak temperature estimated from the alpha-zircaloy layers, which were formed at the shroud wall outer surface during film boiling. Such a temperature estimate was prepared using a temperature-time history similar to that shown in Figure 6. The comparison between the estimated and calculated wall peak temperatures indicates that the molten debris temperature at the time of contact was about 3500 K, which is the same as the temperature calculated from the energy deposition in the test fuel rod at the time of failure (~370 cal/g UO<sub>2</sub>).

The presence of zircaloy in the molten debris strongly influences the transient freezing of the debris. This follows from the fact that the zircaloy thermal properties are higher than those of the UO<sub>2</sub> fuel; that is,  $(\rho_{Zr} C_{Zr} k_{Zr}) > (\rho_{UO_2} C_{UO_2} k_{UO_2})$ . As a result, increasing the zircaloy volume ratio within the debris increases the effective thermal conductivity, and thus accelerates the freezing process and reduces the total freezing time of the molten debris layer. Figure 7 illustrates the effect of the zircaloy volume ratio on the total freezing time of the molten debris layer. As indicated, a four-fold increase in the zircaloy volume ratio (from 10 to 40%) reduced the total freezing time by approximately 50%.

In the previous discussion, the shroud wall did not melt upon being contacted by the molten debris because the temperature of the wall inner surface was less than the melting point of the wall material. In the following subsection the conditions under which wall erosion due to melting could occur are assessed.

### 5.1 Potential Wall Erosion Due to Melting

Figure 8 illustrates the effects of the temperatures of the wall and of the molten debris on the maximum temperature obtainable at the

20

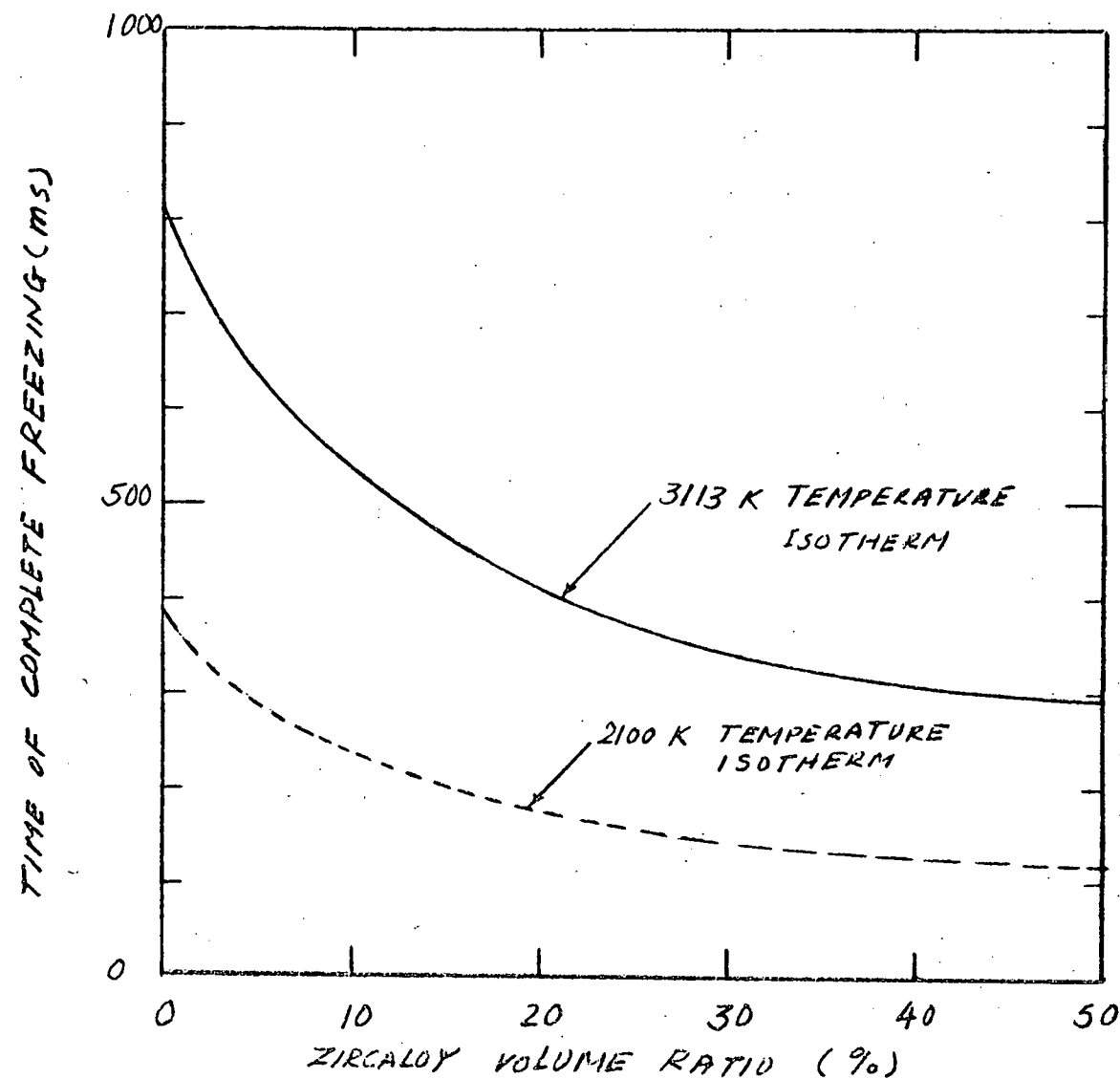


Figure 7. Effect of zircaloy volume ratio within the debris on the total freezing time of the debris layer.

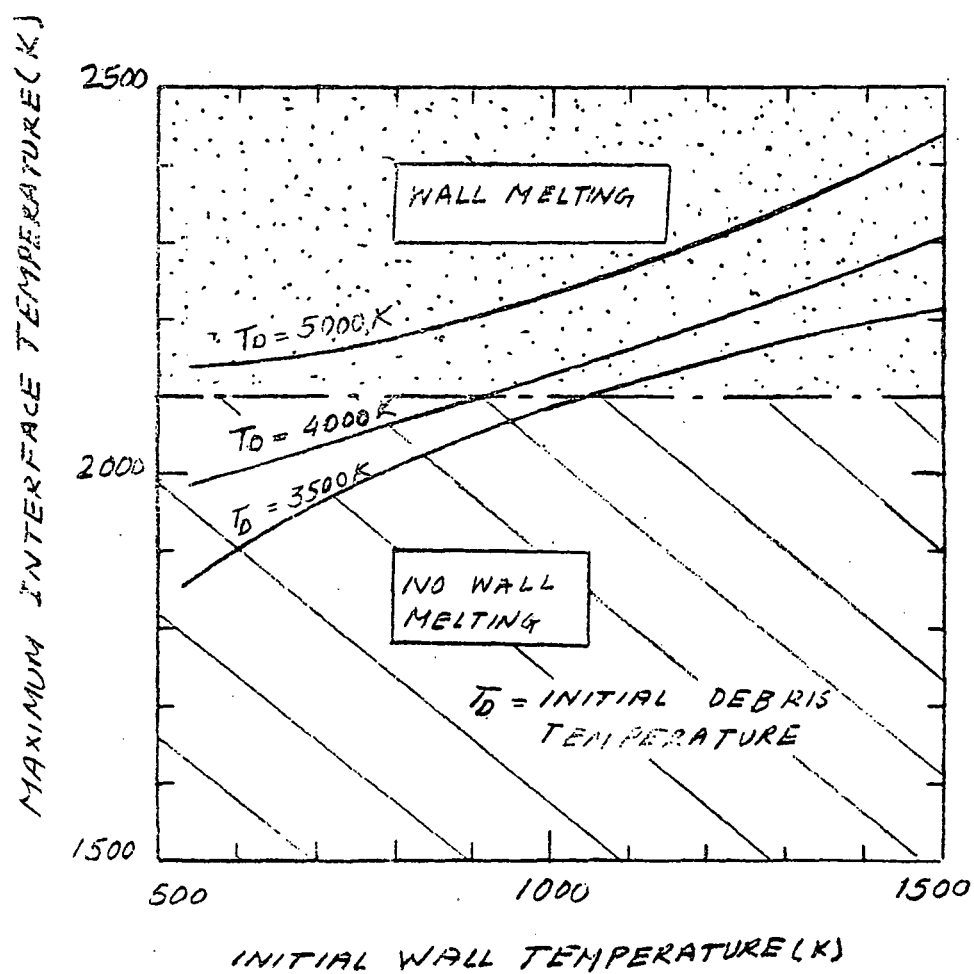


Figure 8. Effects of the wall and the molten debris temperatures at the wall inner surfaces.

inner surface of the wall upon contact. As indicated, melting of the shroud wall would occur if the wall temperature was initially higher than 1000 K or the molten debris temperature was above 4000 K, or both. With those conditions, wall melting and simultaneous freezing of the molten debris would occur. However, the melting process of the wall would be unstable (Figure 9) because of the small thickness of the wall and the continuous cooling at the wall outer surface.<sup>12</sup>

The transient growth and decay behavior of the wall molten layer, when the initial wall temperature is equal to 1500 K, is graphed in Figure 9. As shown, when the molten debris temperature is less than 4000 K, a molten layer grows into the wall until it reaches a maximum thickness (less than the initial thickness of the wall), at which time the conductive heat flux from the frozen debris crust to the wall balances that conducted away through the unmelted region of the wall. Subsequently, the wall molten layer decreases by freezing and eventually disappears. Increasing the molten debris temperature increases the maximum wall melting and the total lifetime of the wall molten layer. As demonstrated in Figure 9, increasing the molten debris temperature from 3500 to 4000 K increases the maximum thickness of the wall molten layer from 37 to 65% of the initial wall thickness and the total lifetime from 2.7 to 4.1 seconds. Complete melting of the shroud wall would occur, however, if the molten debris temperature was equal to or higher than 5000 K.

Noted that the radiation cooling at the debris layer strongly influenced the melting processes of the wall, as shown in Figure 9. Radiation cooling of the debris reduces the heat flux which can be conducted away from the debris layer to the wall, and thus slows down the wall melting process of and decreases the total lifetime of the wall molten layer. In the following subsection, the accuracy of the finite element code (SINGLE) used in the previous calculations is assessed.

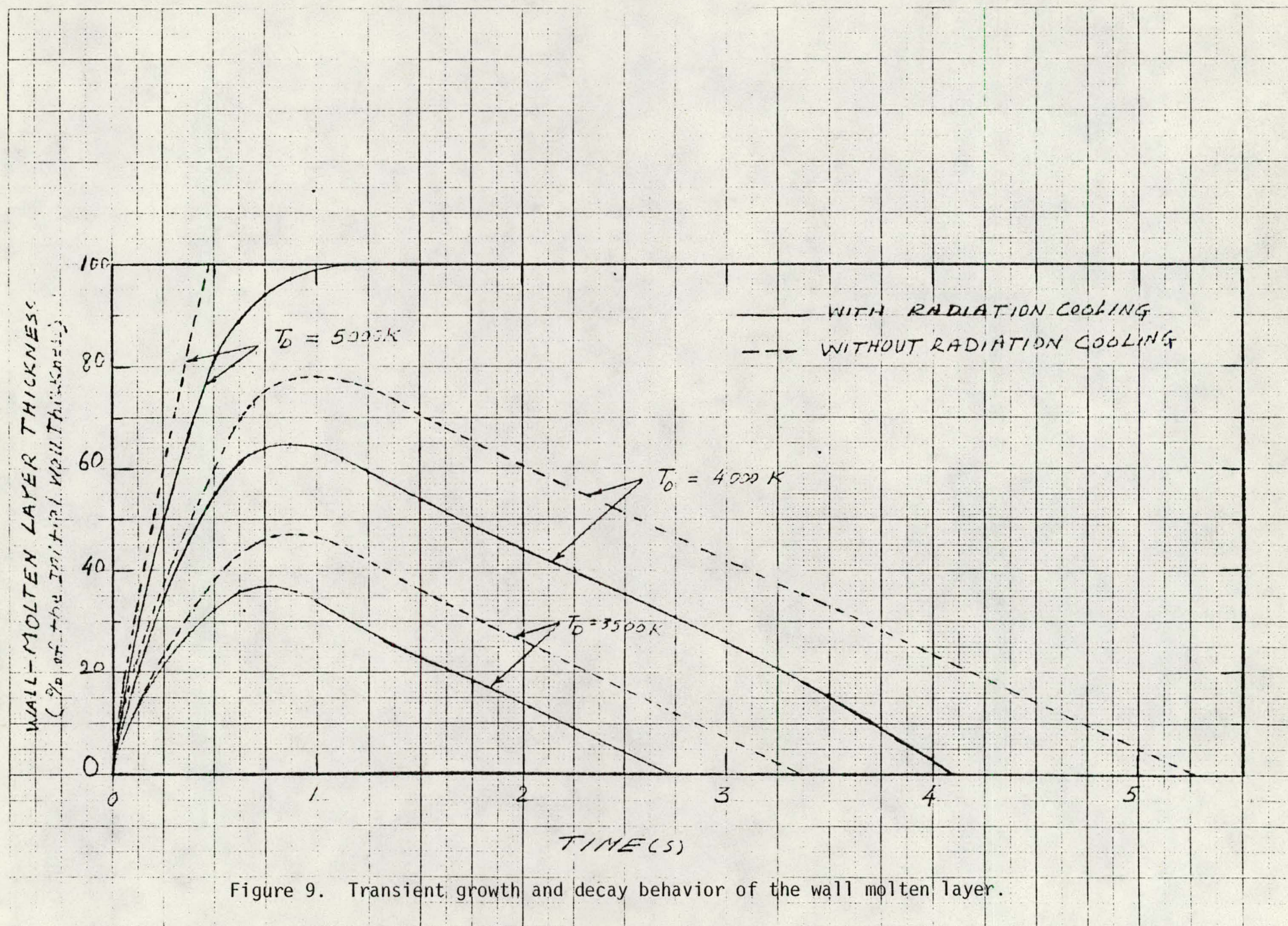


Figure 9. Transient growth and decay behavior of the wall molten layer.

## 5.2 Accuracy of the Finite Element Computer Code SINGLE

The accuracy of the computer code SINGLE in solving transient heat conduction problems with a change-of-phase was examined. The results calculated using the code were compared with the known exact solution to the classical Neumann problem,<sup>13</sup> which pertains to a much less general change-of-phase problem than that explicitly treated in the present work. Assessed is the accuracy of the code when applied to the transient freezing of a stagnant, superheated liquid on an isothermal wall.<sup>13</sup> The freezing constant as obtained by the code and the exact solution is plotted versus the Stefan number for freezing ( $C_s(T_f - T_w)/L$ ) in Figure 10. As shown, the code predictions are accurate to within 2% of the exact solution.

## 6. SUMMARY AND CONCLUSIONS

A reactivity initiated accident in-pile experiment, designated RIA-ST-4, was conducted in the Power Burst Facility at the Idaho National Engineering Laboratory to determine the magnitude of potential pressure pulses as a result of a fuel rod failure during a severe boiling water reactor control rod ejection accident. Extensive amounts of molten debris (primarily a mixture of  $UO_2$  and ziracloy) were produced and expelled axially and radially within the test shroud upon test rod failure (~ 33 ms after the initiation of the burst). A molten debris layer was deposited along the inner surface of the test shroud wall, which had a finite thickness and was continuously cooled at its outer surface by coolant bypass flow. The shroud wall did not melt upon being contacted by the molten debris.

A physical model was developed to parametrically study the transient freezing of the molten debris layer on the inner surface of the RIA-ST-4 test shroud wall, considering the conditions of finite wall thickness, continuous cooling at the wall outer surface, radiation cooling at the debris layer surface, internal heat generation in the debris, and temperature-dependent thermophysical properties. Assessed were the effects of initial debris temperature,

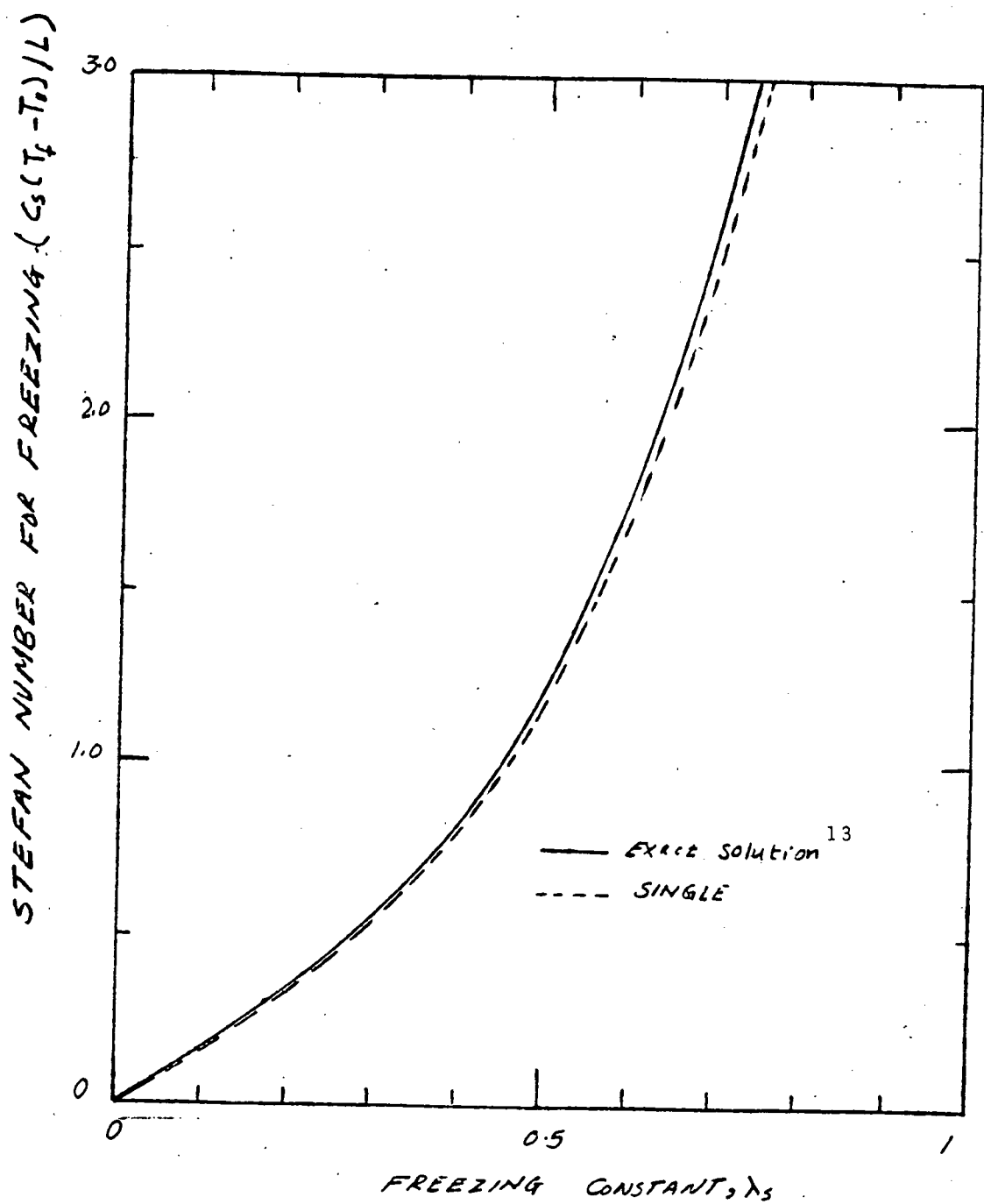


Figure 10. Accuracy of the SINGLE code in calculating the freezing of a superheated liquid on an isothermal wall.

radiation cooling, zircaloy volume ratio within the debris, and initial wall temperature on the transient freezing of the debris layer and the potential melting of the wall upon being contacted by the molten debris. The governing equations of this two-component, simultaneous freezing and melting problem in a finite geometry were solved using a one-dimensional finite element computer code (SINGLE). The code was in good agreement (within 2%) with the known exact solution in calculating the freezing constant of a stagnant, superheated liquid on an isothermal wall.

As indicated, the transient freezing of the molten debris layer was governed by the transient heat conduction through the shroud wall, the initial debris temperature, the radiation cooling of the debris, and the zircaloy volume ratio within the debris. Increasing the initial debris temperature increases the molten debris superheating, which slows down the freezing process and increases the total freezing time of the debris layer. Analysis showed that increasing the zircaloy volume ratio within the debris increases the effective thermal conductivity of the debris, and thus accelerates the freezing process and reduces the total freezing time of the molten debris layer. The calculated temperatures at the shroud wall outer surface were in a fair agreement with the estimated temperatures from the measured thickness of the  $ZrO_2$  and oxygen-stabilized alpha-zircaloy layers. (These layers were formed at the shroud wall outer surface due to the zircaloy-steam reaction during film boiling.) The temperature agreement indicated that the molten debris temperature was about 3500 K at the time of fuel rod failure.

It is concluded that the RIA-ST-4 test shroud wall did not melt because of the low temperatures of the wall (538 K) and of the molten debris (3500 K) at the time of fuel rod failure. Analysis indicated that melting of the shroud wall would occur only if the initial wall temperature was higher than 1000 K, or the molten debris temperature was above 4000 K, or both. However, the melting process of the wall would be unstable under such conditions. The radiation cooling at the debris layer surface strongly influences the transient growth

(melting) and decay (freezing) behavior of the wall molten layer. As indicated, the cooling by radiation, rather than the transient conduction through the wall, cools the debris and reduces the conductive heat flux to the wall, thus slowing down the wall melting and decreasing the total lifetime of the wall molten layer.

## 7. REFERENCES

1. C. L. Zimmerman et al, Experimental Data Report for Test RIA-ST (Reactivity Initiated Accident Test Series), NUREG/CR-0473, TREE-1235 (1979).
2. W. F. Ames, Nonlinear Partial Differential Equations in Engineering, Academic Press, New York (1965).
3. M. S. El-Genk, "On a Vapor Explosion in the RIA-ST-4 Experiment," Trans. of Am. Nucl. Soc. (June 1980).
4. B. K. Larkin and S. W. Churchill, AICHE Journal, 5 (1959) p. 467 .
5. R. L. Gorring and S. W. Churchill, "Thermal Conductivity of Heterogeneous Materials," Chemical Engineering Progress, 57 (1961) pp. 53-59.
6. MATPRO-Version 11, A Handbook of Material Properties for use in the Analysis of Light Water Reactor Fuel Rod Behavior, NUREG/CR-0497, TREE-1280 (1979).
7. W. H. McAdams, Heat Transmission, McGraw-Hill Book Company, New York (1954).
8. L. A. Bromley, "Heat Transfer in Stable Film Boiling," Chemical Engineering Progress, 46, (1950) pp. 221-227.
9. D. P. Jordan, "Film and Transition Boiling," Advances in Heat Transfer, 5, (1968) pp. 55-128.
10. R. E. Pawel, J. V. Cathcart, and R. A. McKee, "The Kinetics of Oxidation of Zircaloy-4 in Steam at High Temperatures," J. Electrochemical Sci. Tech., 126 (July 1978) pp. 1105-1111.

11. R. C. Ballinger, W. G. Dobson, and R. R. Biederman, "Oxidation Reaction Kinetics of Zircaloy-4 in an unlimited steam environment," J. of Nucl. mat., 62, (1976) pp. 213-270.
12. M. S. El-Genk and R. L. Moore, "Freezing and Melting in Finite Media, with an Assessment of Molten Fuel Containment Capability of the SLSF," J. Nucl. Engr. Design, (submitted 1979).
13. H. S. Carslaw and J. C. Jaeger, Conduction of Heat in Solids, 2nd ed., Clarendon Press, Oxford (1959).

## NOMENCLATURE

a,	molten debris layer thickness (m);
b,	shroud wall thickness (m);
B,	time constant ( $s^{-1}$ ), Equation (1);
C,	heat capacity (J/kg·K);
D,	equivalent diameter of the coolant bypass flow, Equation 13,
g,	acceleration of gravity (m/s <sup>2</sup> ), Equation (15),
h,	heat transfer coefficient (W/m <sup>2</sup> ·K);
H,	film boiling length;
$h_{fg}$ ,	latent heat of vaporization (kJ/kg);
k,	thermal conductivity (W/m·K);
L,	latent heat of fusion (J/kg);
Q,	fission heating rate (W/g), Equation (1);
$Q_0$ ,	fission heating rate at time of fuel failure (W/g), Equation (1);
t,	time (s);
T,	temperature (K);
$T_{crit}$ ,	critical temperature of the coolant (K);
$T_f$ ,	fusion temperature (K);
v,	inlet velocity of coolant bypass flow, (m/s), Equation (13);
r,	coordinate (m).

### Greek Letters

$\alpha$ ,	thermal diffusivity (m <sup>2</sup> /s);
$\delta$ ,	frozen debris crust thickness (m);
$\delta_m$ ,	wall molten layer (m);
$\epsilon$ ,	emissivity;
$\mu$ ,	viscosity (kg/ms), Equation (13);
$\sigma_{SB}$ ,	Stefan-Boltzmann constant ( $5.67 \times 10^{-8}$ W/m <sup>2</sup> · K <sup>4</sup> ),

Equations (12) and (15).

$\rho$  density

Subscripts

- a, at the molten debris layer surface ( $r = a$ );
- b, at the shroud wall outer surface ( $r = -b$ );
- B, film boiling;
- c, coolant bypass flow;
- $c_0$ , conduction through the vapor film at the shroud wall outer surface;
- D, molten debris at the time of fuel failure;
- f,  $UO_2$ -fuel, fusion;
- I, at the shroud wall inner surface ( $r = 0$ );
- m, wall molten layer;
- mp, wall melting point;
- r, thermal radiation through the vapor film at the shroud wall outer surface;
- R, radiation cooling at the debris layer surface;
- s, fuel debris layer;
- sat, saturation;
- v, water vapor;
- $UO_2$ , uranium dioxide;
- Zr, zircaloy;
- w, solid wall;
- l, coolant.

